Optoelectronic Materials ISSN 2377–4738 *Optoelectron. Mater. 2 (2017) 53–58*

Effect of LiCl on TiO_2 nanostructures hydrothermally grown on titanium substrate

Song-jie Han[1,2], Xian-kui Lv[1,2], Cheng-xiang Yang[1,2], Kun-peng Gao[1,2], Quan-hong Ou[1,2],Si-lin Zhang[1,2], Li-qiu Zhao[1], Fu-fang Zhou,[1,2,*] Jun-Sheng Shi,[1,2,*]

[1]College of Physics & Electronic Information, Yunnan Normal University, Kunming 650500, P .R. China

[2]Yunnan Key Lab of Opto-electronic Information Technology, Yunnan Normal University, Kunming 650500, P .R. China

(*Received 01 June 2017; accepted 20 September 2017*)

Anatase was synthesized on Ti substrate by one-pot hydrothermal method in tetramethylammonium hydroxide solution, the shape and size of anatase was controlled with doping LiCl. Effects of LiCl on the TiO_2/Ti was characterized by scanning electron microscopy, X-ray diffraction, Raman spectroscopy. The results show that TiO_2/Ti itself without LiCl doping is an ideal material with photocurrent larger in visible than in UV. In addition the one-pot doping method proves to improve the photoelectric properties both in visible and ultraviolet, LiCl doping with 0.02 M for instance has multipled the short-circuit photocurrents in respect with 0 M, even more intriguing: J_{sc} under visible is 3.8 and 3.4 times as much as in ultraviolet.

Keywords: Photoelectric properties; LiCl; Anatase; Hydrothermal synthesis

1. Introduction

It is significant to develop and utilize new energy sources for the modern environment and the human race [1]. With the development of the world economy and energy, solar cells has become a popular approach showing national scientific strength and contribution for humanity. Silicon-based solar cells have already put into commercial production and market operations, [2] but the research needs to go further, given silicon shortcomings, i.e. the high prices and strict production conditions. So the researchers has turned attention to inexpensive environmentally friendly anatase TiO_2 solar cells in the last century [3].

Anatase TiO_2 can be used in many fields: materials for solar cells which may work under any light conditions; [4] a photocatalyst that can degrade and convert part of unfriendly environment substances; [5] a self-cleaning materials incorporated into a coating, [6] and so on. According to the application, there are different methods to prepare TiO_2 in the laboratory around world. Common methods are hydrothermal method[7], sol-gel method[8], surface guide[9], electrospinning[10], chemical vapor deposition[11], reverse micelles method[12] and so on.

TiO_2 are broadband gap semiconductors, needing energy larger than 3.2eV to excite electron-hole pairs, in other words, only the UV light, a small part of sun lights is able to be converted into electric power on the TiO_2. To improve the photoelectric efficiency, metal ions doping is frequently used for better properties of solar cells,[18] for doping creates doping bands to decrease the request of incident light energy. In the field of solar cells, in the past and currently, TiO_2 electrode always attract intense interests, from dye-sensitized solar cells to nowadays research hot spot perovskite solar cells, TiO_2 supporting is an optimum select electrode. [19, 20] So discovering and understanding more of its features is valuable.

Extensive efforts have been devoted to develop innovative synthesis strategies for nanomaterials in order to exploit the true potential of nanotechnology.[13] Hydrothermal generation of TiO_2 is a simple, low-cost process suitable for industrial scale use. Here we present a novel approach to produce LiCl doped TiO_2 anatase structures from Ti substrate by one-pot hydrothermal method, where TMAOH reacts with Ti in aid of H_2O. TMAOH is a strong organic base, used for a lot of organic synthesis[14,15,17]. As well known $Ti(OBu)_4$, a usual precursor to synthesize TiO_2, meanwhile TiO_2 layer was formed and was guided in ordered arrays during deposition in the solution [14]. When $(TMAO)^-$ was selected in stead of $(OBu)^-$, it also can direct synthesis of TiO_2 in tetramethylammonium hydroxide solution, surrounding Ti (as the source of TiO_2), serving as a structure template in the synthesis solution. It is fantastic to find that Ti/TiO_2 electrodes yield more photocurrents in visible than in UV lights.

2. Experiment

2.1 Ti plate preparation

The titanium plate(99.99%, 0.01mm) was cut with a size of 1.5cm*2.5cm, cleaned the grease stains on surface with alcohol.Then they were dipped and cleaned by ultrasonic cleaning in alcohol, acetone, distilled water for 5 minutes respectively, dried in the oven at 70℃ for half an hour.

2.2 Solution preparation

Four aqueous solution of 0.3 mol/L TMAOH was prepared, and they were added respectively 0 mol/L, 0.01 mol/L, 0.02 mol/L, 0.03 mol/L LiCl, stirred to mix well. Each of prepared solution were taken 30ml into the clean interior of one autoclave respectively.

2.3 Crystal preparation

Two pieces of Ti were put into each solution in the autoclaves, the oven temperature was maintained at 200 ℃ for 12 h. Then subsequently decreased to room temperature over 3 h, the pieces of as grown TiO_2/Ti were ultrasonically washed in alcohol, acetone, distilled water for 10 minutes respectively.

2.4 Characterization

*Corresponding author. Email: ffz144@126.com, shi-js@263.net

Surface morphology is investigated by scanning electron spectroscope (SEM), phase structure and crystal form is obtained at 40mV-36mA from X-ray diffractometer (XRD, Bruker D8) using Cu Kα radiation at room temperature. Confocal microscope Raman spectrometer (Invia, Renishaw Corp., U.K.) is used to obtain Raman spectra. Uv-vis spectra are recorded on an U-4100 PC spectrometer (Hitachi. Japan). The photoelectrochemical properties of the samples were studied by means of cyclic voltammetry. It was investigated in three-electrode system with the aid of electrochemical workstation (CHI660E), the working electrode, counter electrode and reference electrode was respectively the measured sample, Pt and mercury oxide.

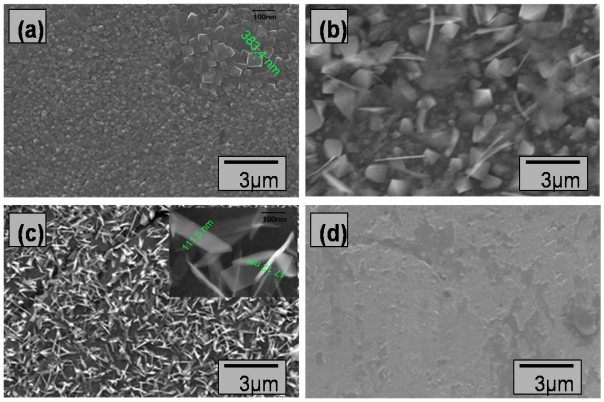

Fig. 1 XRD SEM images of samples obtained with different concentration of LiCl in 0.3 mol/L TMAOH: (a) without LiCl, (b) 0.01 mol/L, (c) 0.02 mol/L, (d) 0.03mol/L.

3. Results and discussions

3.1 SEM images of prepared samples

The SEM images of surface morphology of samples were shown in Fig.1, exhibiting the concentration of LiCl effects on the formation of TiO_2 on Ti substrate. As shown in Fig.1 (a), without LiCl, TiO_2 are mainly clusters of bipyramidal rods,[17] with average 300-400 nanometers, not exceeding four hundred nanometers. According to literature, [17] the Ti substrate can produce bipyramidal anatase crystal in the TMAOH solution. With concentration 0.01 mol/L, as showed in Fig.1 (b), there appeared numerous large nanoribbons of about 2-3 μm wide, 10nm thick vertically edge-on among bipyramidal rods. And it is worth noting that bipyramidal rod tips, analogous to those Fig.1 (a), vertically on the titanium substrate, as wide as 600-700nm, were coexistent as well. Up to 0.02mol/L, zonal TiO_2 nanoribbons on Ti substrate appear in (c), the nanosheets are only a dozen or tens of nanometers thick, whereas about 350-700 nanometers wide. At LiCl 0.03mol/L showed in (d), the fundamental nano- or micro-structures of the crystal on substrate surface has almost disappeared. The remnant structures in Fig.1(d) suggests that extra LiCl amount results in break-off of self-assembling equilibrium reaction process of TiO_2 anatase.

Observed from the surface morphologies of TiO_2, nanostructures can be affected significantly by concentration of LiCl from 0-0.03 mol/L in 0.3 mol/L TMAOH aqueous solutions. Further on, the size and shape of nanocrystal can be controlled with LiCl.

As discussed in the literature, the mechanism of TiO_2 formation in TMAOH is assumed as: those organic ions are arranged in accordance with certain rules in the Ti surface to induce the formation of TiO_2 crystals. TiO_2 crystals are thus guided to grow, perpendicular to the substrate surface, along certain preferential orientation, therein forming preferential special facets[14], taking a principle as to reduce surface energy more [17]. However, owing to the addition of Li^+ and Cl^-, they impact the configuration of TMA^+ ions and the bonding of $Ti\text{-}OH^-$ in solution system.

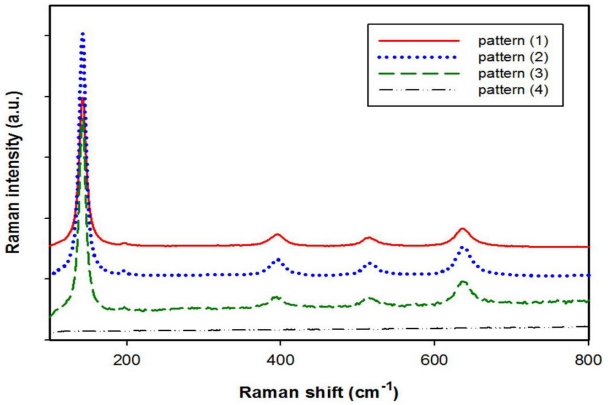

Fig. 2 Raman spectra of the samples obtained by hydrothermal process in 0.3 mol/L TMAOH aqueous solutions with different concentration of LiCl: (a) without LiCl, (b) 0.01 mol/L, (c) 0.02 mol/L, (d) 0.03mol/L.

3.2 Raman spectroscopy

Raman spectroscopy represents the vibration mode of atom relative position changes in sample surface molecules. Groups in molecules have their own characteristic vibration peaks, the composition of sample surface materials can be determined by the position of peaks. Fig.2 shows the Raman spectra of the samples obtained by hydrothermal process in TMAOH aqueous solutions with different concentration of LiCl. Raman scattering spectrum (1), (2) and (3) in Fig.2 displays $143cm^{-1}$,$197cm^{-1}$,$392\ cm^{-1}$,$510cm^{-1}$, $633\ cm^{-1}$ peaks, in accord with the peak positions in the reference [14], which are the characteristics of crystalline anatase. There is few peaks in spectrum (4) in Fig.2. according to literature. [17] Considering the areas applied to measurement are the same for the four samples, the anatase content follows the Raman scattering intensity order as: (4)<(1)<(3)<(2). Our work proved that the shape and scale of the products can be controlled on nanoscale both for nanopillars and nanoribbons via adding LiCl in the reaction solution. There is no peak in pattern (4) of Fig.2 arising from excessive LiCl.

3.3 The X-ray diffraction

Through carrying out X-ray diffraction on the material and analyzing its diffraction pattern, information about the composition of material and about structure or shape of the atoms or molecules inside the material can be obtained. Fig.3 shows the XRD patterns for the samples prepared by hydrothermal process in 0.3mol/L TMAOH aqueous solutions with different concentration of LiCl on

Ti substance. The concentration of LiCl is respectively (1) 0mol/L, (2) 0.01mol/L, (3) 0.02mol/L, (4) 0.03mol/L. Visually, the peak positions of the three lower concentrations in Fig.3 are extremely similar. It is seen that the XRD data for the samples match with the standard diffraction data from JCPDS files 21-1272, 44-1294 for anatase and titanium, respectively. XRD pattern (4) consists with standard Ti as JCPDS No. 44-1294. From this aspect, perfect anatase is formed in the LiCl concentration in the regime of 0-0.02mol/L, but higher concentration is not suitable for feasible optoelectronic materials. There is not significant evidence that degree of orientation, this might seem some contradictory with the fact in Fig.1(c), where exist numerous side-edged nano-ribbons. So we assume side-edged nano-ribbons should be dispersed only near the surface. In addition, there is only anatase in Fig.3 (a), this indicates anatase film is thick enough, at least 100 nm, formed a homogenous coverage on Ti substrate. From (b) to (c) anatase and Ti co-exist, and in (d) only Ti can be observed.

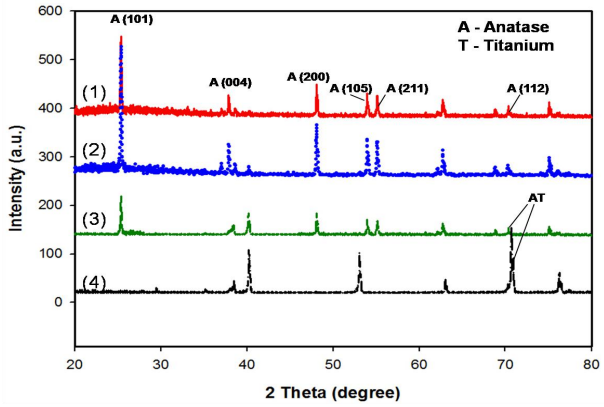

Fig. 3 XRD patterns for the samples prepared by hydrothermal process in 0.3mol/L TMAOH aqueous solutions with different concentration of LiCl on Ti substance. The concentration of LiCl is respectively (1) 0mol/L, (2) 0.01mol/L, (3) 0.02mol/L, (4) 0.03mol/L.The photoelectric properties

3.4 The photoelectric properties

To investigate the performance of TiO_2/Ti films as photoelectrodes, cyclic voltammetry techniques were used, the results shown in Fig.4, the photocurrent of samples of TiO_2/Ti films obtained from Ti substrate by hydrothermal in TMAOH aqueous solution with LiCl of (1) 0 M, (2) 0.01 M, (3) 0.02 M. Under visible light illumination 80.4 mW/cm^2 (a) or ultraviolet light illumination 19.6 mW/cm^2 irradiation (b). Short circuit photocurrents and open circuit voltage of the samples from Fig.4 are listed in Table 1.

As showed in Fig. 4 (a), in the case of visible irradiation, evidently the photocurrent increases with LiCl concentration within 0-0.02 M. LiCl Doping improves photoelectric properties while looking at this aspect of photocurrent. For photocurrent of 0.02 M LiCl is approximately four times of that without LiCl. As for in the case of UV irradiation shown in Fig. 4 (b), the tendency of photocurrent with LiCl concentration is similar with that of 4 (a), different is just 0.02 M is about 3.4 times of that 0 M LiCl.

It is worth mention from information in Fig. 4 and Table 1 that 0 M LiCl itself is an ideal material with photocurrent larger in visible than in UV even if in normalized irradiation powers. Supposing that photocurrent scales with irradiation power, consider the power ratio of visible-to-UV being only 4.1, but the visible-to-UV ratio of short circuit photocurrent for 0 M LiCl is 5.8. Thus the photoelectric conversion efficiency is higher for visible light than for UV in 0 M LiCl anatase TiO_2 film. Similarly the visible-to-UV ratio of short circuit photocurrent for 0.01 M and 0.02 M LiCl is 4.3, 6.4 respectively. From the perspective of photocurrent J_{SC}, photoelectric conversion efficiency in the increased order is 0.01 M<0 M < 0.02 M LiCl.

It is interesting to find that there is a large variation in V_{OC} for 0, 0.01, 0.02 M LiCl under visible light, in contrast to almost a constant in UV. Apparently, only 0.01 M gains in the V_{OC}, meanwhile 0.02 M appears not so in favor of V_{OC}.

Relating Voc, we have below equation:

$$V_{OC} = \frac{kT}{q} \ln\left(\frac{J_{SC} N_D \tau_{eff}}{q n_i^2 d}\right) \quad (1)$$

where k is the Boltzmann constant, T is the temperature, q is elemental charge, J_{SC} is short-circuit current density, N_D is the doping concentration, τ_{eff} is the effective carrier recombination lifetime, n_i is the intrinsic carrier concentration and d is the thickness of the light absorber. Herein taking eq(1) in application, we could get Table 2. For example, now we examine the impact of 0.02 M LiCl referred to 0 M in visible light: T, q, n_i is the same; J_{SC} is 4.1 multipled; and we have reasonable grounds to believe d is getting thinner, for 0.03 M LiCl already leads to destruction of almost any structures of anatase, presented in earlier XRD and Raman sections. From the fact that XRD intensity of anatase (101) planes for 0.02 M LiCl is roughly double that of 0 M, assuming that d decreased to half of the anatase thickness of 0 M, meanwhile taking into mind that their V_{OC} is much the same, so $N_D \tau_{eff}$ of 0.02 M LiCl is only 1/8 of 0 M LiCl.

Though actual doping concentration is unknown, N_D with 0.02 M LiCl doping in any case should not be lowered than that of 0 M, hence τ_{eff} is much lowered for 0.02 M LiCl than for 0 M. The reasoning above related is credible, and now the conclusion makes sense, since doping always generate multitudinous defects, which lead to lower τ_{eff}.

In other words, significantly higher efficiencies with concentration of LiCl can reasonably be explained by the LiCl optimizing the size and shape of the single crystal nanostructure. It is even more noteworthy that photocurrents of all samples under visible light illumination is greater than the photocurrent under ultraviolet light at normalized power, which is an solid evidence of improving photoelectric performance in the visible light region by adjustment of LiCl concentration.

3.5 The UV-Vis absorption spectroscopy

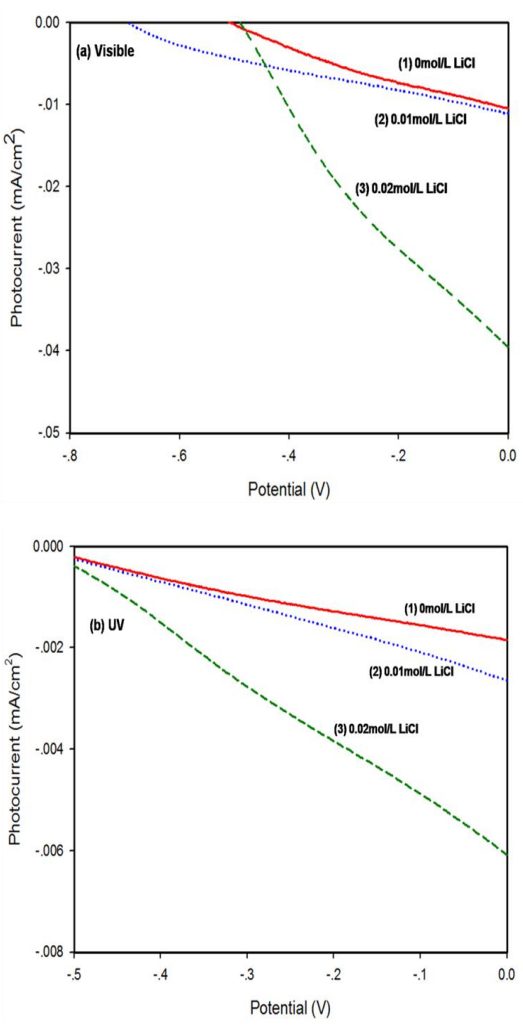

Fig. 4 Photocurrents under visible (80.4 mW/cm^2) and UV (19.6 mW/cm^2) irradiation of samples obtained from Ti substrate hydrothermally in 0.3mol/L TMAOH aqueous solution with LiCl of (1) 0 M, (2) 0.01 M, (3) 0.02 M. Aqueous electrolyte was Na_2S/NaOH/S (1:1:1 molar ratio)

Uv-vis absorption spectroscopy used ultraviolet visible near infrared spectrophotometer U-4100 made by the Japanese Hitachi. As shown in Fig.5, undoped TiO_2 in Fig. 5 (a) possesses a distinct upslope of intensity starting at about 370 nm (characteristic absorption edge of bulk TiO_2 being 380 nm), uprising from the broad terrace herewith longer wavelength until 800 nm. Taking into consideration that anatase composes a small amount of the TiO_2/Ti, referred to the results discussed in XRD section, the 370 nm upslopes in Uv-vis absorption spectra demonstrates the existence of TiO_2.

Focusing this position of 370 nm, the protrusion of intensity relatively decreases with concentration of LiCl from (a) 0 M, (b) 0.01 M to (c) 0.02 M, until disappearing in (d) 0.03 M. This gives evidence of that excessive LiCl destructs the formation of anatase single crystals.

On the other hand, from 0 M to 0.02 M each has wide band absorption in visible region, manifesting a wide gentle terrace from 370 up to 800nm. 0.03 M LiCl in Fig.4 (d) is an exception, not only there is hardly any protrusion at about 370 nm, but also with a dome in its wide-band absorbance centering at about 500nm. The difference may be related to the surface composition as discussed in XRD results, it is composed of almost Ti. The ridge at about 500nm may come from the remnant structures shown in Fig.1(d), it seems that the excessive LiCl in TMAOH aqueous solution results in interruption of self-assembly of TiO_2 anatase.

Table 1. Photocurrents of samples under UV and visible illumination

Sample No.	Concentration (M)	Photocurrent J_{SC} (mA /cm^2)		Open-circuit Voltage V_{OC} (V)	
		UV light	Visible light	UV light	Visible light
1	0	0.18×10^{-2}	1.04×10^{-2}	0.55	0.50
2	0.01	0.26×10^{-2}	1.11×10^{-2}	0.55	0.67
3	0.02	0.61×10^{-2}	3.93×10^{-2}	0.53	0.49

Table 2. Ratio of V_{OC}, J_{SC}, d, N_D, τ_{eff} with respect to 0 M

Sample No.	Concentration	UV light				Visible light			
	(M)	V_{OC}	J_{SC}	**d**	$N_D\tau_{eff}$	V_{OC}	J_{SC}	**d**	$N_D\tau_{eff}$
1	0	1	1	1	1	1	1	1	1
2	0.01	1.0	1.4	1.6	1/0.9	1.3	1.1	1.6	1/5.3
3	0.02	1.0	3.4	0.5	1/6.8	1	3.8	0.5	1/8

Thus it can be observed that the doped TiO_2 possess higher absorption than none-doped one visible light region. For the three lower concentrations of doped LiCl, the absorption in the visible region is even higher than the ultraviolet ranges, this is especially worth noting, and might open a new train of thought to create more

preferable electrode materials for solar cells, exploiting visible light more efficiently. Furthermore, this series of materials may have surprisingly excellent performs for light catalytic role [15].

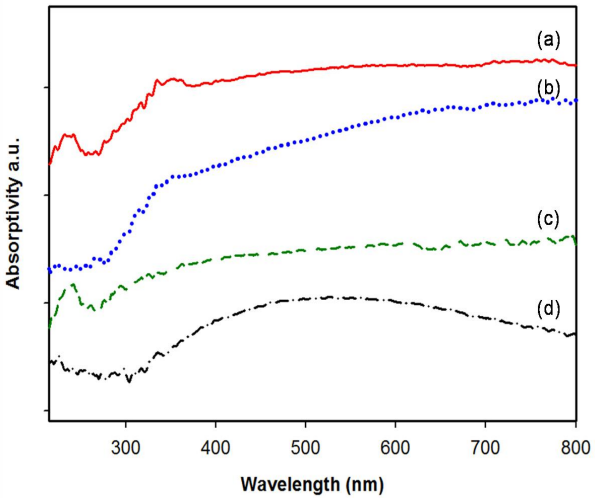

Fig. 5 T Uv-Vis Absorption Spectroscopy of Samples with LiCl of (a) 0 M, (b) 0.01 M, (c) 0.02 M, (d) 0.03 M

4. Conclusions

Anatase was synthesized on Ti substrate by one-pot hydrothermal method in tetramethylammonium hydroxide solution, the shape and size of anatase was controlled with doping LiCl. Effects of LiCl on the TiO_2/Ti was characterized by scanning electron microscopy, X-ray diffraction, Raman spectroscopy. The preparing method proved to improve the photoelectric properties. The short circuit photocurrents of the as-prepared sample with 0.02 M LiCl are more than three times higher than that without LiCl both under UV and visible irradiation, in addition to that, at a visible-to-UV incident illumination power ratio of 4.1, the ratio of visible-to-UV short circuit photocurrent is 5.8, 4.3 and 6.4, respectively for 0, 0.01 and 0.02 M LiCl, thus the conversion efficiency was improved significantly by LiCl doping. Facts prove that the TMAOH-Ti reaction produces excellent TiO_2/Ti electrode for solar cells, even more interesting, one-pot hydrothermal doping markedly improved J_{sc}, more significant in visible than in UV.

Acknowledgment

This research was supported by the National Natural Science Foundation of China (No. 61166005, 61178054), Doctoral Startup Fund of Yunnan Normal University (2016zb016), and Yunnan Provincial Education Branch Research Fund (2011Y306, 2012Y171).

References

[1] M. Grätzel, Dye-sensitized solar cells. Photochemistry reviews, *Journal of Photochemistry and Photobiology C* 4 (2003) 145–153.

[2] C. Xiao, X. Yu, D. Yang, D. Que, Impact of solar irradiance intensity and temperature on the performance of compensated crystalline silicon solar cells, *Solar Energy Materials and Solar Cells* 128 (2014) 427–434.

[3] X. Chen and S. S. Mao, Titanium dioxide nanomaterials: Synthesis, properties, modifications, and applications, *Chemical Reviews* 107 (2007) 2891-2959.

[4] C. Cui, Y. Qiu, J. Zhao, B. Lu, H. Hu, Y. Yang, N. Ma, S. Xu, L. Xu, X. Li, A comparative study on the quantum-dot-sensitized, dye-sensitized and co-sensitized solarcells based on hollow spheres embedded porous TiO_2 photoanodes, *Electrochimica Acta* 173 (2015) 551–558.

[5] V. Etacheri, C. D. Valentin, J. Schneider, D. Bahnemann, S. C. Pillai, Visible-light activation of TiO_2 photocatalysts: Advances in theory and experiments, *Journal of Photochemistry and Photobiology C* (2015) 1–29.

[6] A. Bozzia, T. Yuranovaa, I. Guasaquilloa, D. Laubb, J. Kiwia, Self-cleaning of modified cotton textiles by TiO_2 at low temperatures under daylight irradiation, *Journal of Photochemistry and Photobiology A* 174 (2005) 156–164.

[7] J. Yu, G. Wang, B. Cheng, M. Zhou, Effects of hydrothermal temperature and time on the photocatalytic activity and microstructures of bimodal mesoporous TiO_2 powders, *Applied Catalysis B: Environmental* 69 (2007) 171–180.

[8] A. Katoch, H. Kim, T. Hwang, S. S. Kim, Preparation of highly stable TiO_2 sols and nanocrystalline TiO_2 films via a low temperature sol–gel route, *Journal of Sol-Gel Science and Technology* 61 (2012) 77-82.

[9] S. Zhu, S. Liang, Q. Gu, L. Xie, J. Wang, Z. Ding, P. Liu, Effect of Au supported TiO_2 with dominant exposed {001} facets on the visible-light photocatalytic activity. *Applied Catalysis B: Environmental* 119–120 (2012) 146–155.

[10] H. Huang, Y. Jie, C. Wang, Synthesis of LiCl doped hollow TiO_2 nanofibers via electrospinning and their humidity-sensing properties, *Advanced Materials Research* 476-478 (2012) 1116-1120.

[11] P. Hájková , P. Špatenka, J. Krumeich, P. Exnar, A. Kolouch, J. M atoušek, P. Kočí, Antibacterial effect of silver modified TiO_2/PECVD films, *The European Physical Journal D* 2 (2009) 189-193.

[12] K. Elghniji, M. Ksibi, E. Elaloui, Sol-gel reverse micelle preparation and characterization of N-doped TiO_2: Efficient photocatalytic degradation of methylene blue in water under visible light, *Journal of Industrial and Engineering Chemistry* 18 (2012) 178–182.

[13] X. Wang, H. Wang, Y. Zhou, Y. Liu, B. Li, X. Zhou & H. Shen, Confined-space synthesis of single crystal TiO_2 nanowires in atmospheric vessel at low temperature: a generalized approach, *Scientific Reports* 5 (2015) 8129.

[14] M. Jafari, A. Nouri, M. Kazemimoghadam, T. Mohammadi, Investigations on hydrothermal synthesis parameters in preparation of nanoparticles of LTA zeolite with the aid of TMAOH, *Powder Technology* 237 (2013) 442–449.

[15] Y. Chen, X. He, X. Zhao, Q. Yuan, X. Gu, Preparation, characterization, and growth mechanism of a novel aligned nanosquare anatase in large quantities in the presence of TMAOH, *Journal of Colloid and Interface Science* 310 (2007) 171–177.

[16] Y. B. Ryub, M. S. Leeb, E. D. Jeongc, H. G. Kimc, W. Y. Junga, S. H. Baeka, G. D. Leea, S. S. Parka, S. S. Honga, Hydrothermal synthesis of titanium dioxides from peroxotitanate solution using different amine group-containing organics and their photocatalytic activity, *Catalysis Today* 124 (2007) 88–93.

[17] X. Dong, J. Tao, Y. Li, H. Zhu, Oriented single crystalline TiO_2 nano-pillar arrays directly grown on titanium substrate in

tetramethylammonium hydroxide solution, *Applied Surface Science* 256 (2010) 2532–2538.

[18] Y. Lv, Y. Li, H. Sun, Y. Guo, Y. Li, J. Tan, X. Zhou, Yttrium-doped TiO 2 nanorod arrays and application in perovskite solar cells for enhanced photocurrent density, *Thin Solid Films* 651 (2018) 117-123.

[19] Z. Zhang, L.Xie, R. Lin, Q. Qin, Y. Cai , Y. Zhou, H. Liu, X. Lu, X. Gao, L. Shui, S. Wu, J.-M. Liu, Enhanced performance of planar perovskite solar cells based on lowtemperature processed TiO_2 electron transport layer modified by Li_2SiO_3, *Journal of Power Sources* 392 (2018) 1-7

[20] K. S. Anuratha, H.-S. Peng, C.-K. Hsieh b , Y. Xiao, J.-Y. Lin, Electrochemical formation of TiO_2 porous layer for perovskite solar cells, *Thin Solid Films* 660 (2018) 720-724